Dynamic-warping full-waveform inversion to overcome cycle skipping

M. Wang[1], Y. Xie[1], W. Q. Xu[1§], K. F. Xin[1#], B. L. Chuah[1], F. C. Loh[1], T. Manning[2], S. Wolfarth[2],*
[1] CGG, [2] BP, [§]presently Goldman SACHS, [#]presently PETRONAS

Summary

In this paper we develop dynamic-warping full-waveform inversion (D-FWI) to address the well-known cycle skipping problem in conventional full-waveform inversion (FWI). The dynamic warping technique is used to detect the traveltime difference between the predicted and the observed data. We make use of the timeshift to partially warp the observed data and thus generate a series of datasets that connect the predicted and the observed data. We then use the modified observed data to solve a sequence of conventional FWIs that avoid the cycle skipping issue. Synthetic and real data examples show that D-FWI can converge successfully by overcoming the cycle skipping problem, while conventional FWI results in an erroneous model. With this new approach, we can invert velocity models starting from a higher frequency and/or a poor starting model. This technology has the potential to save time in the processing sequence since it allows the velocity model building to start with minimum pre-processing on the seismic data and to be done in parallel with other pre-processing steps.

Introduction

FWI is widely used in the exploration industry for generating high-resolution and high-fidelity velocity models which can significantly improve migration results and even provide direct information about the reservoir (Sirgue et al., 2009; Ratcliffe et al., 2011). However, because of the highly oscillatory nature of seismic data, resulting in an inherent strong nonlinearity of the objective function, the conventional FWI, which is based on minimizing the least-squares difference between the predicted and observed data, often suffers from numerous local minima. This so-called cycle skipping problem occurs when the difference in the arrival time between the predicted and the observed data is larger than a half cycle of the dominant frequency (for example, see Virieux and Operto, 2009). A multi-scale frequency sweeping method (Bunks et al., 1995), which fits data components sequentially from low to high frequency, is often proposed to avoid cycle skipping. The success of this frequency sweeping approach relies strongly on some potentially demanding prerequisites, including an accurate initial model and sufficiently low frequency components in the seismic data. In the processing of field data, seismic data below 3 to 4 Hz is often unavailable due to acquisition limitations and noise contamination. On the other hand, traveltime tomography, which is often used to provide an initial velocity model for FWI, has its own limitations, especially for near surface data where limited offsets are available for residual moveout analysis in the common image gathers.

As a consequence, a lot of effort has been devoted to mitigating, or resolving, the cycle skipping issue in conventional FWI. For example, several papers have tried to address the issue of mismatched events between the predicted and observed data: Luo and Schuster (1991) exploited the convex property of traveltime in waveform inversion; Ma and Hale (2013) applied the dynamic warping technique from Hale (2013) to recover the traveltime difference between the observed and the predicted data and then updated the velocity model by minimizing this traveltime difference; Luo and Hale (2013) also used dynamic warping to measure the traveltime difference between the observed and predicted data but then expanded the observed data about the warped timeshifts to form a residual without cycle skipping in a conventional waveform inversion scheme; Warner and Guasch (2014) used Wiener filters to measure the wavefield difference and push the predicted data towards the observed one by punishing filter coefficients with large time-lag.

We propose a new method, D-FWI, to tackle the cycle skipping problem. First we use the dynamic warping technique (Hale, 2013) with constraints to detect the traveltime difference between the predicted and the observed data. We then apply the timeshift to the observed data with different scales and thus generate a series of datasets that connect the predicted and the observed data. Finally, we use the modified observed data in the framework of conventional FWI and solve a sequence of inversions that avoid the cycle skipping problem. As the predicted data progressively converges to the observed data, the updated velocity model converges to the true model as well. We demonstrate our method using the well-studied 2D Marmousi model and a real data example from Indonesia. In both cases, our method successfully overcomes the cycle skipping problem and provides good velocity models, while conventional FWI converges to an erroneous result.

Method

Conventional FWI's objective is to minimize the least-squares difference between the predicted and the observed data

$$f = \left\| P_M - D \right\|^2, \qquad (1)$$

where D is the observed data and P_M is the synthetic data predicted by the model M. When the initial model M is far from the correct one, conventional FWI cannot converge from P_M to D when there is a lack of low frequency signal in the seismic data. In fact, cycle skipping occurs when the maximum time difference between the predicted and the observed data is larger than a half cycle of the dominant frequency. To solve this issue we propose to generate a series of datasets satisfying the following two conditions: 1) connecting the predicted and the observed data, 2) constraining the maximum time difference between two adjacent ones in the series to be less than a half cycle of the dominant frequency. Then we propose to solve a sequence of conventional FWIs

$$f_n = \|P_M - D_n\|^2, \quad (2)$$

where D_n are the generated datasets connecting the observed and the predicted data.

To produce the connecting series, we first need the information of the time difference between the predicted and the observed data. This can be provided by the robust dynamic warping algorithm (Hale, 2013). Dynamic warping searches for temporal and spatial variant timeshifts τ to minimize the least-squares difference between the predicted and the shifted observed data

$$C(\tau) = \|P_M(x_r, x_s; t) - D(x_r, x_s; t + \tau(x_r, x_s; t))\|^2 \quad (3)$$

with the constraints of

$$\left|\frac{\partial \tau}{\partial t}\right| \le \sigma_t \quad \left|\frac{\partial \tau}{\partial x_s}\right| \le \sigma_s \quad \left|\frac{\partial \tau}{\partial x_r}\right| \le \sigma_r,$$

where x_r is the location of receivers, x_s is the location of shots and the σ's are the maximum values allowed in each domain. With the constrained optimization, dynamic warping can avoid cycle skipping for band-limited data and estimate the timeshifts accurately.

After estimating the maximum of the modulus of the time difference, $\Delta t_m = \max\{|\tau(x_r, x_s; t)|\}$, we can now define an integer N by

$$N = \min\left\{ n \,\middle|\, \frac{\Delta t_m}{n} < \frac{T}{2} \right\}, \quad (4)$$

where T is the duration of one cycle of the dominant frequency in the seismic data. In practice, a safety factor is applied to get N. A series of bridging datasets are defined

$$D_n(x_r, x_s; t) = D\left(x_r, x_s; t + \left(1 - \frac{n}{N}\right)\tau(x_r, x_s; t) \right). \quad (5)$$

The modified data will be used in conventional FWI. For instance, in the first round FWI will try to invert for the velocity which makes the predicted data P_M move towards the shifted observed data D_1. By construction, there is no cycle skipping between P_M and D_1 since their maximum time difference is less than the half cycle of the dominant frequency according to equations (4) and (5).

In summary, we generate a series of modified observed datasets where no cycle-skipping occurs. We move the predicted data towards the observed data step by step along the generated series. With this proposed D-FWI algorithm we can achieve a reasonable velocity field when starting from higher frequency and/or a poor starting model.

Examples

To demonstrate our method, we first use the well-known 2D Marmousi model. As shown in Figure 1(a), we modified the velocity model by adding a 200 m thick water layer on the top of the original Marmousi model. For simplicity, constant density is used to generate the synthetic data and in the inversion as well. Figure 1(b) shows the one dimensional initial model with the correct water velocity and a linearly varying velocity profile from water bottom to the lower boundary of the model. The shots and receivers are arranged uniformly with a grid spacing of 24 m and a depth also of 24 m. The maximum offset used in FWI is 5 km. The water surface is set as a free surface to model ghosts and free-surface multiples. We ran the inversion iteratively from 3 to 10 Hz using diving waves, reflections and their multiples. The total number of iterations is 110 (1/5 of the shots are used in each iteration). The water velocity is kept fixed during the inversion process. All the parameter settings are exactly the same for both conventional FWI and D-FWI. At 3Hz, a significant portion of the data predicted by the initial model is cycle skipped. It can be seen from Figure 1(c) that conventional FWI is unable to recover the correct model and the subsurface geological structures are significantly distorted, especially on the right-hand side. On the other hand, the result in Figure 1(d) shows that D-FWI successfully copes with cycle skipping and inverts a velocity model which is closer to the true one.

We also applied D-FWI on a real dataset to illustrate the effectiveness of this new approach. This is an Indonesian 3D OBC survey acquired in shallow water and a strong current environment. There are carbonate layers in the shallow section around 1 km in depth. We used FWI to obtain a shallow target velocity model. Both conventional FWI and D-FWI were executed through frequencies from 3.5 to 5 Hz with 20 iterations in total. Here only the diving waves out to the maximum offset of 3 km are used to update the shallow velocity model. The initial velocity, shown in Figure 2(a), is a manually sped up velocity model according to existing geological information. However, cycle skipping still exists between the observed data in Figure 3(a) and the synthetic data in Figure 3(b), which is predicted by this initial velocity model. The corresponding

shot location is indicated by the yellow arrow in Figure 2(a). Due to cycle skipping, conventional FWI inverted a low velocity at ~1 km in depth as shown in Figure 2(b). The corresponding synthetic data shown in Figure 3(c) is very different from the observed data. In comparison, D-FWI can mitigate cycle skipping and figure 2(c) shows that D-FWI has a high velocity layer at the expected depth level. The synthetic data generated by D-FWI is shown in Figure 3(d). It is much closer to the observed data. We ran depth migration using these three velocity fields to check their effects on the image. Figure 4 displays one inline section going through the carbonate area. Pull-ups exist in the conventional FWI result in figure 4(b) due to the wrong inverted velocity. The D-FWI results in figure 4(c) show

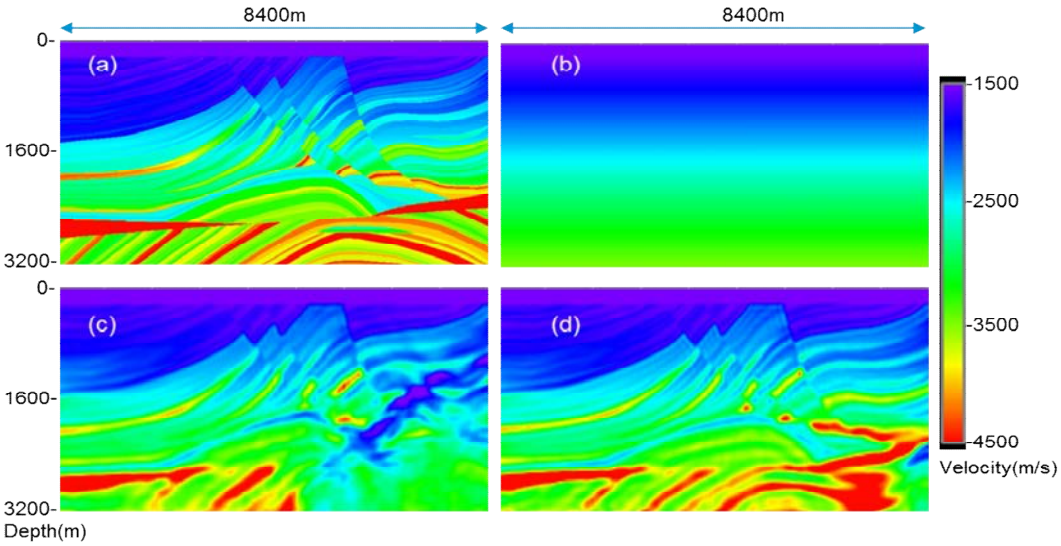

Figure 1: (a) The true Marmousi model with an additional 200 m water layer. (b) A one-dimensional initial model with correct water velocity. (c) Result from conventional FWI from 3 to 10 Hz. (d) Result from D-FWI from 3 to 10 Hz. We can see that D-FWI successfully overcomes the cycle skipping issue, while conventional FWI fails to recover the correct model in places.

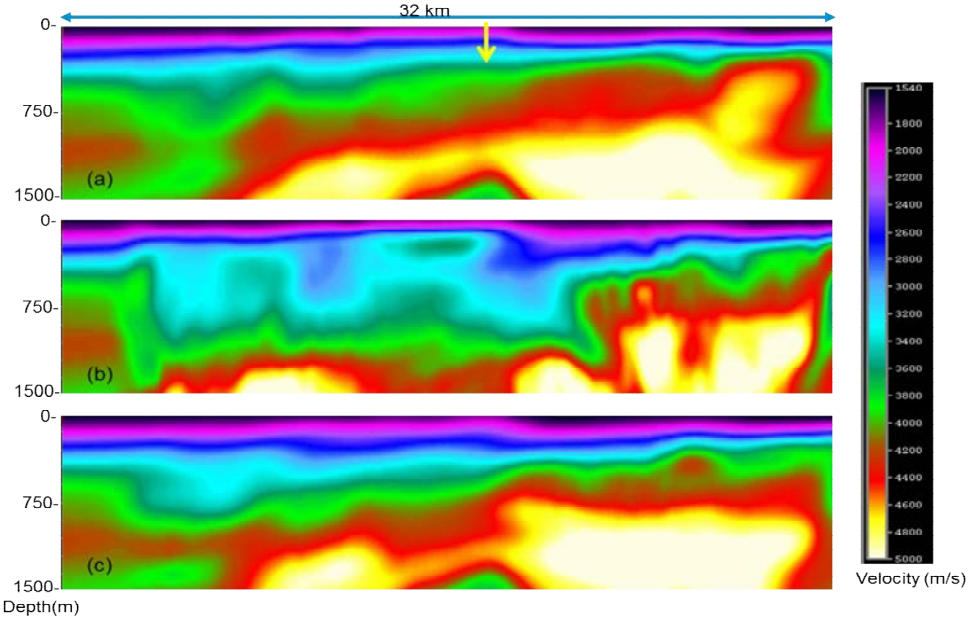

Figure 2: (a) Initial velocity model which is manually sped up to include the carbonate feature at ~1 km depth. (b) Velocity model of conventional FWI from 3.5 to 5 Hz. (c) Velocity model of D-FWI from 3.5 to 5 Hz.

better event focusing in the shallow, as well as the deep, section compared with the initial velocity results. Since we only updated the velocity up to 5Hz with limited iterations and offset range, additional passes of FWI based on the current D-FWI results can be run to further improve the velocity model.

Conclusions

Dynamic-warping FWI makes use of traveltime difference information provided by the dynamic warping technique to reconstruct a series of effective observed datasets that are free of cycle skipping. As the flow moves on, the modified observed data will converge to the original observed data and the updated velocity model converges to the true model. As demonstrated through the synthetic and real data examples, our new technique is capable of inverting for a reasonable velocity model starting from higher frequency and/or a poor initial model, while conventional FWI suffers from cycle skipping problems and fails to converge to the correct velocity model.

Acknowledgments

The authors would like to thank CGG and BP for permission to publish this work and BP, Tangguh partners, SKKMIHAS, and MIGAS to show the data examples. Appreciation is given to Xiaoning Yue and Tao Lin for their technical support and Jiangtao Hu for his testing. The authors would like to thank Dechun Lin and Joe Zhou for their valuable suggestions for this work. Thanks go to Andrew Ratcliffe, Gilles Lambare, Thomas Hertweck and Barry Hung for the paper review and all the suggestions.

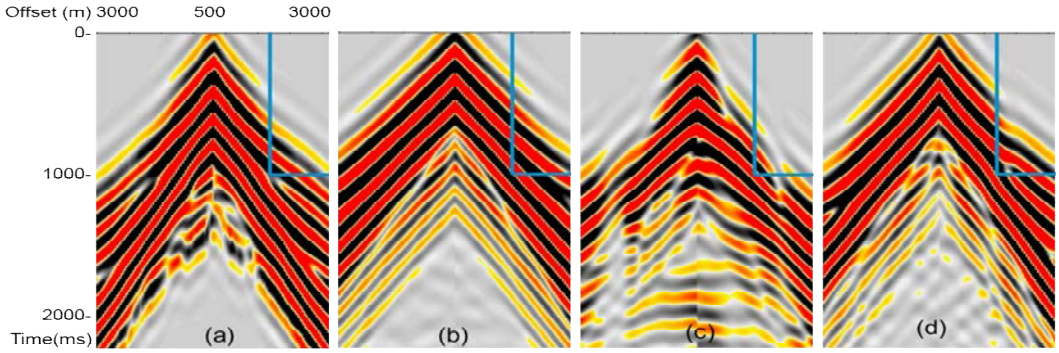

Figure 3: The observed data (a) and synthetic datasets predicted by: (b) initial model, (c) conventional FWI updated model and (d) D-FWI updated model. All of them have been filtered with a low-pass of 5 Hz. We can see that the initial model has a cycle skipping issue compared with the observed data, meaning conventional FWI fails to move the modeled data in the correct direction. In comparison, D-FWI results in a much better fit with the observed data.

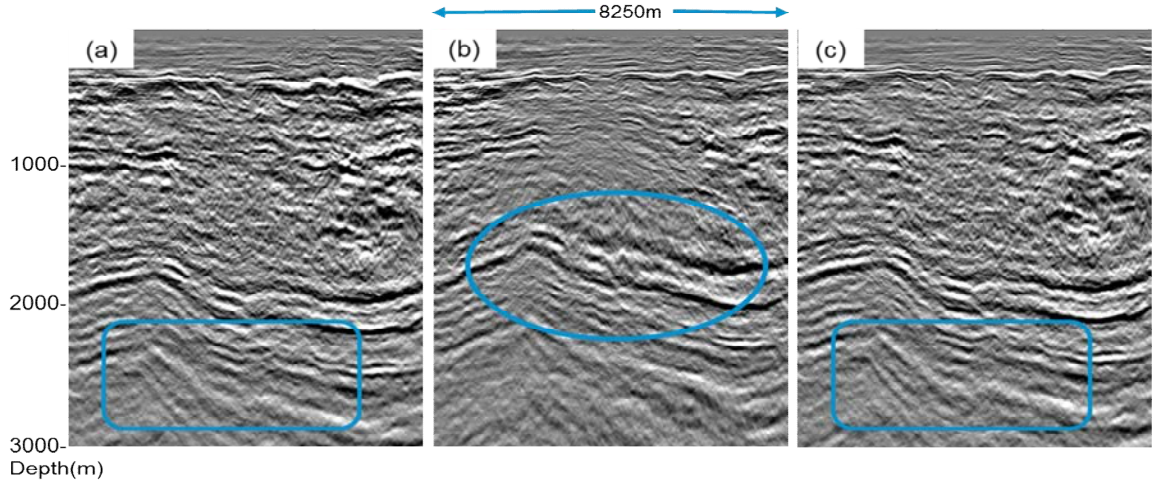

Figure 4: 3D depth migration stack section of one inline going through the shallow carbonate layer: (a) results of initial velocity, (b) results of conventional FWI, and (c) results of D-FWI. Pull-ups still exist, or are made worse, in conventional FWI due to the wrong velocity, whereas the image is improved with D-FWI.

EDITED REFERENCES

Note: This reference list is a copyedited version of the reference list submitted by the author. Reference lists for the 2016 SEG Technical Program Expanded Abstracts have been copyedited so that references provided with the online metadata for each paper will achieve a high degree of linking to cited sources that appear on the Web.

REFERENCES

Bunks, C., F. Saleck, S. Zaleski, and G. Chavent, 1995, Multiscale seismic waveform inversion: Geophysics, **60**, 1457–1473, http://dx.doi.org/10.1190/1.1443880.

Hale, D., 2013, Dynamic warping of seismic images: Geophysics, **78**, no. 2, S105–S115, http://dx.doi.org/10.1190/geo2012-0327.1.

Luo, S., and D. Hale, 2013, Separating traveltimes and amplitudes in waveform inversion: 83rd annual meeting, SEG, Expanded Abstracts, 969–974.

Luo, Y., and G. T. Schuster, 1991, Wave-equation traveltime inversion: Geophysics, **56**, 645–653, http://dx.doi.org/10.1190/1.1443081.

Ma, Y., and D. Hale, 2013, Wave-equation reflection traveltime inversion with dynamic warping and full-waveform inversion: Geophysics, **78**, no. 6, R223–R233, http://dx.doi.org/10.1190/geo2013-0004.1.

Ratcliffe, A., C. Win, V. Vinje, G. Conroy, M. Warner, A. Umpleby, I. Stekl, T. Nangoo, and A. Bertrand, 2011, Full waveform inversion: A North Sea OBC case study: 81st Meeting, SEG, Expanded Abstracts, 2384–2388, http://dx.doi.org/10.1190/1.3627688.

Sirgue, L., O. I. Barkved, J. P. van Gestel, O. J. Askim, and J. H. Kommendal, 2009, 3D waveform inversion in Valhall wide-azimuth OBC: 71st Meeting, EAGE, Expended Abstracts, U038, http://dx.doi.org/10.3997/2214-4609.201400395.

Virieux, J., and S. Operto, 2009, An overview of full-waveform inversion in exploration geophysics: Geophysics, **74**, no. 6, WCC1–WCC26, http://dx.doi.org/10.1190/1.3238367.

Warner, M., and L. Guasch, 2014, Adaptive Waveform Inversion – FWI without Cycle Skipping – Theory: 76th Meeting, EAGE, Expended Abstracts, We E106 13, http://dx.doi.org/10.3997/2214-4609.20141092.